Structural Basis for the Improved Drug Resistance Profile of New Generation Benzophenone Non-Nucleoside HIV-1 Reverse Transcriptase Inhibitors†

Jingshan Ren,[‡,¶] Philip P. Chamberlain,[‡,¶] Anna Stamp,[‡] Steven A. Short,[§] Kurt L. Weaver,[§] Karen R. Romines,[§] Richard Hazen,[§] Andrew Freeman,[§] Robert G. Ferris,[§] C. Webster Andrews,[§] Lawrence Boone,[§] Joseph H. Chan,[§] and David K. Stammers*[,‡]

Division of Structural Biology, The Wellcome Trust Centre for Human Genetics, Henry Wellcome Building for Genomic Medicine, University of Oxford, Roosevelt Drive, Oxford, OX3 7BN, U.K., and GlaxoSmithKline Inc., 5 Moore Drive, Research Triangle Park, North Carolina 27709

Received April 21, 2008

Owing to the emergence of resistant virus, next generation non-nucleoside HIV reverse transcriptase inhibitors (NNRTIs) with improved drug resistance profiles have been developed to treat HIV infection. Crystal structures of HIV-1 RT complexed with benzophenones optimized for inhibition of HIV mutants that were resistant to the prototype benzophenone GF128590 indicate factors contributing to the resilience of later compounds in the series (GW4511, GW678248). Meta-substituents on the benzophenone A-ring had the designed effect of inducing better contacts with the conserved W229 while reducing aromatic stacking interactions with the highly mutable Y181 side chain, which unexpectedly adopted a "down" position. Up to four main-chain hydrogen bonds to the inhibitor also appear significant in contributing to resilience. Structures of mutant RTs (K103N, V106A/Y181C) with benzophenones showed only small rearrangements of the NNRTIs relative to wild-type. Hence, adaptation to a mutated NNRTI pocket by inhibitor rearrangement appears less significant for benzophenones than other next-generation NNRTIs.

Introduction

Non-nucleoside inhibitors of reverse transcriptase (NNRTIs[a]) are part of certain multidrug regimens used in the treatment of HIV infection.[1] In spite of the achievements of combination therapy in reducing the deaths from AIDS in Western countries, continued treatment of HIV infection is likely to be compromised by the emergence and spread of drug resistant virus. It is thus important that novel drugs are developed that are active against HIV that has mutated to escape the selection pressure from current antiretroviral therapies. Three virus specific proteins, reverse transcriptase (RT), protease, and gp41 are important targets for currently approved anti-HIV drugs. Additionally, a CCR5 virus coreceptor antagonist and an HIV integrase inhibitor have recently been approved for treatment of HIV infection.[2] The majority of approved anti-HIV drugs, however, act as inhibitors of reverse transcriptase, the enzyme that has a central role in virus replication. The larger subunit of the RT p66/p51 heterodimer contains two distinct inhibitor sites one of which binds nucleotide analogue inhibitors (NRTIs) and a second that binds non-nucleoside inhibitors (NNRTIs).[3,4] NRTIs, compete with analogous nucleotide substrates and following incorporation into the primer strand, act as DNA chain terminators.[5] NNRTIs bind in an allosteric pocket that is ~10 Å from the polymerase active site and inhibit RT by distorting the catalytically essential aspartic acid residues.[6,7] To date, four NNRTIs have been approved for clinical use: nevirapine (NVP) and delavirdine (DLV) (Scheme 1) are classified as first generation NNRTIs, while efavirenz (EFV) (Scheme 1), which shows greater resilience to the presence of drug resistance mutations, is classified as a second generation inhibitor.[1,8,9] A wide range of chemically diverse compounds have been identified as NNRTIs; yet there is a common theme in their interaction with RT involving a conserved "two-ring" binding mode. In spite of this related binding feature there are, however, subtle NNRTI-dependent differences in the conformation of the drug-binding pocket itself as shown when comparing a range of crystal structures.[10−15] Previous studies of structures of drug resistant mutant RTs in complex with NNRTIs have indicated the basis for drug resistance.[16−22]

The emergence of resistance to current anti-HIV drugs in clinical use means that further compounds are required in order to allow continued suppression of the viral infection. To this end we are developing novel NNRTIs that have greatly improved resistance profiles thereby retaining activity against most current clinically relevant HIV mutants resistant to this drug class. Structure−activity data for optimization of initial benzophenones such as **1** (GF128590[23]) have been described in previous publications leading to **2** (GW69564[24]), **3** (GW678248[25,26]), and its prodrug **4** (GW695634 [25]) (Scheme 1). Compounds such as **2** and **3** show a greatly improved profile of activity against mutant HIV resistant to existing approved drugs such as NVP and EFV (Scheme 1, Figure 1). Studies of resistance development by passaging HIV in vitro with escalating levels of **3** have revealed that two sets of three mutations are selected under different conditions: (V106I, E138K, P236L and K102E, V106A, P236L).[27] A set of three mutations appeared necessary to give significant drug resistance for **3**.

Our strategy for developing new generation benzophenone NNRTIs with improved resilience to current drug resistant HIV has included combining medicinal chemistry methodology

† Coordinates and structure factors for the six HIV-1 RT-benzophenone wild-type and mutant structures reported here have been deposited in the PDB. The codes are as follows: 3DLE, 3DLG, 3DM2, 3DMJ, 3DOK, 3DOL.

* To whom correspondence should be addressed. Phone: +44-1865-287-565. Fax: +44-1865-287-547. E-mail: daves@strubi.ox.ac.uk.

‡ University of Oxford.

¶ These authors contributed equally to the work.

§ Glaxo Smith Kline Inc.

[a] Abbreviations: RT, HIV reverse transcriptase; NNRTI, non-nucleoside reverse transcriptase inhibitor; NRTI, nucleoside reverse transcriptase inhibitor; NVP, nevirapine; DLV, delavirdine; EFV, efavirenz; CPV, capravirine (S-1153); ETV, etravirine (TMC-125).

10.1021/jm8004493 CCC: $40.75
Published on Web 07/30/2008

Scheme 1

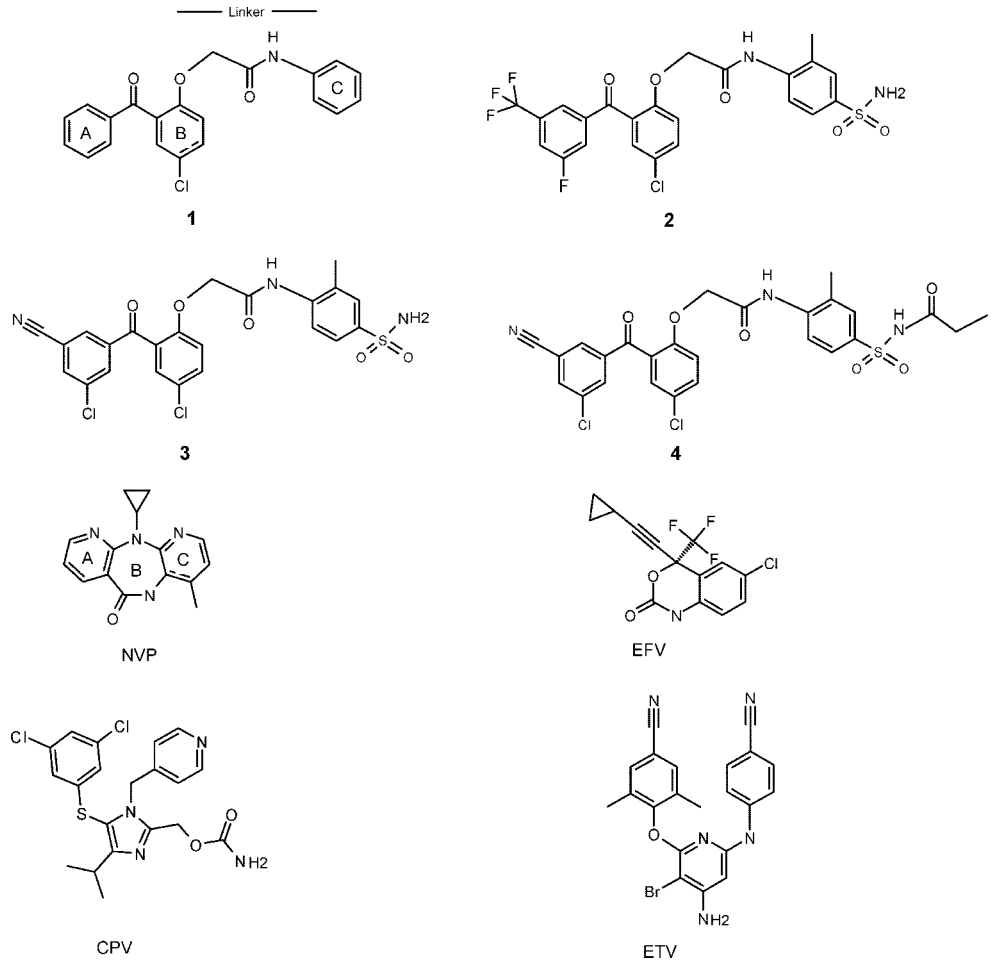

together with crystallographic structure determination of RT−inhibitor complexes.[24] Previous examples of the use of crystallographic approaches for NNRTI design include the development of emivirine analogues,[28] novel quinolones,[29,30] and the ETV NNRTI series.[31]

Structures of prototype benzophenones bound to HIV-1 RT such as **1** were initially determined and used to assist in defining regions of the inhibitor amenable to modification. Further cocrystal structures of newly synthesized compounds were used to assess binding modes. Such an approach has particular benefits for a flexible protein such as RT, where the prediction of inhibitor binding modes can be less than straightforward. Indeed, unexpected protein conformational shifts were observed for complexes containing later members of the benzophenone series that appear to be significant in explaining their resilience. Thus, as well as contributing to the inhibitor design strategy, the structural work has been able to identify factors that can explain the greatly improved resistance profile of later stage benzophenones such as **2** and **3** compared to prototype compounds. Such principles reported here may have wider applications in developing further novel NNRTIs from different chemical series.

Results and Discussion

Anti-HIV-1 Profile of 1. The activity of the prototype unsubstituted benzophenone **1** has only been reported against wild-type and a limited range of HIV-1 mutants.[23] To allow comparison of the drug resistance profile of **1** with later members of the benzophenone series (**2**, **3**[24,26]), its potency was determined in antiviral assays covering a wide range of 24 known drug resistant mutant viruses. To allow directly comparable data, compounds **2** and **3** and the reference drugs (NVP, DLV, EFV) were tested against the same panel of mutant HIV viruses. For the latter five compounds very similar data were obtained compared to that from earlier work on these NNRTIs. [24−26] The data show that **1** has significant loss of potency against single point mutations such as those at codons 181, 188, and 106, while there is a more modest loss against the important K103N mutant (Figure 1, Supporting Information Table 1). Large decreases in potency are seen with seven out of the eight double mutants tested. Overall, **1** has a resistance profile characteristic of a first generation NNRTI such as NVP, while **2** and **3** have markedly superior retention of activity against a wide range of mutations.

RT-Benzophenone Structure Determination. Details of the X-ray data collection and the refinement statistics are shown in Table 1. A total of 14 structures of benzophenones in complexes with wild-type and various mutant RT proteins were determined during the course of this project. However, for this present report in the interests of brevity, we describe a subset of six protein−ligand complexes that we regard as the most relevant for illustrating key features to understanding the drug resistance profile of different compounds. These six RT−NNRTI structures consist of a prototype benzophenone with a relatively poor drug resistance profile, **1**, bound to wild-type RT; a late stage compound **2** in complexes with wild-type and two mutant RTs (K103N and V106A-Y181C); and the final stage clinical

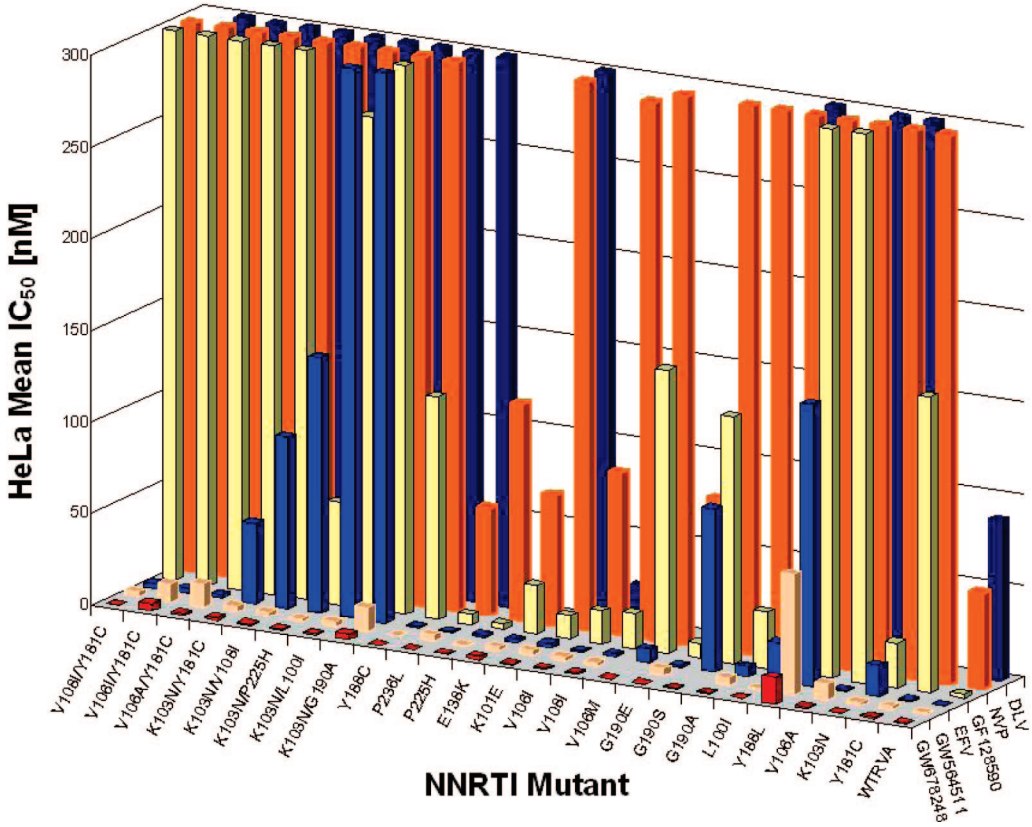

Figure 1. Comparison of the potencies of selected benzophenones and approved NNRTI drugs (DLV, NVP, EFV) against wild-type and a panel of NNRTI- resistant mutant HIV in tissue culture. Note that the IC_{50} values depicted for DLV exceeded 2000 nM with RT mutants P236L, K103N/L100I, K103N/P225H, K103N/V108I, K103N/Y181C, and V106A/Y181C. For NVP, it exceeded 2000 nM for Y181C, K103N, Y188L, G190A, G190S, V106M, K103N/G190A, K103N/L100I, K103N/P225H, K103N/V108I, K103N/Y181C, V106A/Y181C, V106I/Y181C, and V108I/Y181C, and this value exceeded 2000 nM with **1** against the Y188L mutant.

Table 1. Statistics for Crystallographic Structure Determinations

data collection details						
data set	WT-GF128590	WT-GW4511	K103N-GW4511	V106A-Y181C GW4511	K103N - GW678248	L100I -GW695634
data collection site	SRS PX7.2	ESRF ID14EH3	ESRF ID14EH3	ESRF ID14EH3	ESRF ID14-2	SRS PX9.6
wavelength (Å)	1.488	0.931	0.931	0.931	0.933	0.870
unit cell (*a*, *b*, *c* in Å)[a]	137.9, 110.2, 72.4	137.2, 109.5. 72.2	135.9, 109.2, 71.4	137.2, 109.0, 71.9	136.9, 109.8, 72.5	139.0, 111.5, 73.0
resolution range (Å)	30.0−2.5	30.0−2.2	30.0−3.1	30−2.6	30.0−2.9	30.0−2.5
observations	126 633	293 059	40 409	221 843	202 274	555 157
unique reflections	37 308	54 861	17 958	33 883	24 821	40 079
completeness (%)	95.8	97.9	90.2	99.8	99.9	100
average $I/\sigma(I)$	17.5	22.7	6.1	14.6	13.2	27.6
R_{merge}[b]	0.046	0.057	0.119	0.084	0.105	0.120
outer resolution shell						
resolution range (Å)	2.59−2.5	2.28−2.2	3.21−3.1	2.69−2.6	3.0−2.9	2.64−2.5
unique reflections	3277	5084	1882	3310	2443	3942
completeness (%)	85.7	92.3	86.9	99.2	97.6	100
average $I/\sigma(I)$	3.1	1.3	0.6	1.3	1.2	2.1
refinement statistics						
resolution range (Å)	30.0−2.5	30.0−2.2	30.0−3.1	30.0−2.6	30.0−2.9	30.0−2.5
no. of reflections (working/test)	35418/1863	52028/2769	16809/859	32154/1679	23568/1203	37992/1988
R factor[c] (R_{work}/R_{free})	0.214/ 0.296	0.220/ 0.299	0.221/0.307	0.197/ 0.284	0.218/0.312	0.224/0.288
no. atoms (protein/ inhibitor/water)	7711/26/129	7659/36/224	7656/36/0	7656/36/63	7703/34/8	7739/38/115
rms bond length deviation (Å)	0.008	0.007	0.007	0.007	0.012	0.008
rms bond angle deviation (deg)	1.3	1.4	1.4	1.4	1.8	1.4
mean *B* factor (Å^2)[d]	54/58/37/46	55/61/40/47	60/66/51/−	56/62/46/41	73/78/59/68	63/68/52/59
rms backbone *B* factor deviation (Å^2)	4.2	5.1	4.5	4.8	6.9	6.6

[a] All crystals belong to space group $P2_12_12_1$.[41,42] [b] $R_{merge} = \sum|I - \langle I\rangle|/\sum\langle I\rangle$. [c] *R* factor $= \sum|F_o - F_c|/\sum F_o$. [d] Mean *B* factor for main chain, side chain, inhibitor, and water molecules.

candidate **3** with K103N RT as well as its prodrug form **4** with L100I RT. The resolution varies among these structures; that with **2** bound to wild-type RT is the highest in this work at 2.2 Å resolution (Figure 2).

Overall Binding Mode of Benzophenones to HIV-1 RT. Pointers for Drug Design. The mode of binding of the different benzophenones to RT has the A-ring placed in the top hydrophobic pocket that is lined by the aromatic residues Y181,

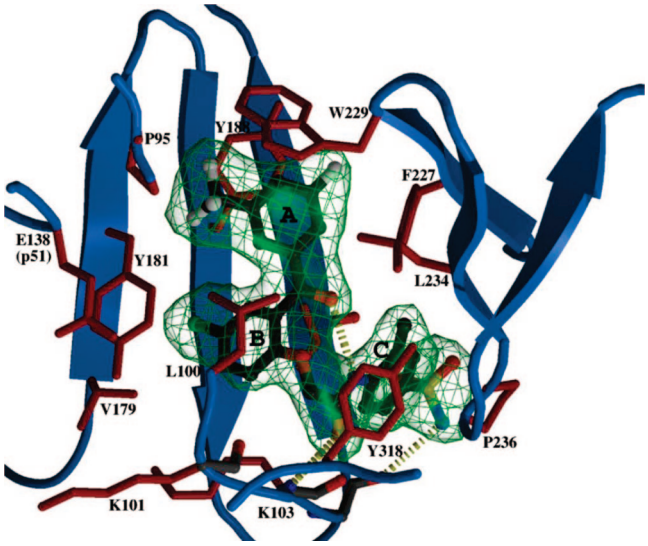

Figure 2. Compound **2** bound in the NNRTI site showing the electron density from the simulated annealing omit $f_o - f_c$ map at 2.2 Å resolution; contouring is at 4σ. The protein backbone is drawn as a schematic colored blue; side chains that interact with **2** are colored red. The inhibitor is shown as ball and stick and is colored by atoms. Hydrogen bonds are shown as broken lines. The three rings of the benzophenone are labeled A, B, C. The electron density is contoured with a chicken wire surface colored green.

Y188, and W229. The A-ring of **2** also forms van der Waals contacts with L234 (via a CD atom) and F227 (CB atom). Dependent on the particular member of the series, variations in the positioning of the side chain of Y181 are observed. A typical NNRTI-bound "up" position is seen for Y181 in the RT complex with the prototype benzophenone **1**, while a "down" position is found in complexes with **2**−**4**, more typical of unliganded RT. Such changes appear significant for understanding the resistance profiles of each compound (see section below). The B-ring is sandwiched between the side chains of L100 and V106, the latter making van der Waals contacts with the inhibitors (Figure 3a). As a result of Y181 adopting a "down" position, it forms interactions with the chloro substituent on the B-ring of **2** via the CB atom and with V179 via a CG atom. The interaction of the chloro substituent with the main-chain carbonyl of Y188 is maintained. The C-ring is located toward a solvent accessible region that forms one entrance to the NNRTI pocket, with contacts being formed on either side by the side chains of V106 and P236. An unusual feature of the benzophenone series is the presence of an internal hydrogen bond linking the carbonyl group between the A and B rings with the NH group of the linker joining rings B and C (Scheme 1, Figures 2 and 3a). Such an intramolecular hydrogen bond has not been previously reported for other NNRTI series when bound to RT. The presence of this hydrogen bond may be entropically favorable for binding, as it could help restrain the inhibitor conformation in solution to be similar to that in the RT bound state. A number of hydrogen bonds between the inhibitor and protein main chain are present; in the case of **2** these involve residues K103, K104, and V106 (Figures 2 and 3a).

The RT-bound structure of initial members of the benzophenone series pointed to a number of features that aided in the design of further analogues. First, it was apparent that there was space in the top subpocket of the NNRTI binding site to accommodate substitutions on the A-ring. Introduction of meta-substituents could improve contact of the A-ring with the side chain of W229 while reducing interactions with the side chain of residue Y181. The potential advantage of this switch is the highly conserved nature of W229,[32] while Y181 is readily mutated. For the benzophenone B-ring, while it is possible to introduce further substituents, such increase in bulk will result in tighter packing and thus more likelihood of a single point mutation giving high level resistance. The location of one end of the C-ring close to the entry point of the NNRTI pocket and thus accessible to solvent looked suitable for the addition of hydrophilic substituents aimed at improving water solubility.

Comparison of the Binding Mode of 2 with a Prototype Benzophenone 1. Overlaying the structures of RT in complexes with a prototype unsubstituted benzophenone, **1**, and an optimized compound **2** reveals interesting differences (Figure 3a). Certain of these observed changes had been predicted, while other features were not anticipated. First, introduction of meta-substituents onto the A-ring of **1** had the desired effect of shifting the A-ring higher up into the hydrophobic top subpocket and establishing van der Waals contacts with the highly conserved W229 side chain. In doing so, it was hoped that the aromatic ring stacking interactions, particularly with Y181, would be reduced while compensating the loss of binding energy by formation of new contacts with W229. In fact and unexpectedly, the inhibitor ring stacking contacts with Y181 were more drastically reduced than anticipated by virtue of the fact that Y181 adopted a "down" position with the tyrosine hydroxyl group having undergone a shift of >10 Å (Figure 3a). The internal hydrogen bond was retained within both **1** and **2** as well as for all other benzophenone inhibitors studied.

Comparison of Benzophenone Binding Modes with Those of NVP and EFV. The binding mode of the benzophenone NNRTIs to RT shows some significant differences from that for current drugs NVP and EFV (parts b and c of Figure 3). The position of the A-ring of **2**, although lying in almost the same plane as the NVP A ring, is significantly shifted by 2.9 Å. The keto group connecting the benzophenone A and B rings lines up with the edge of the NVP B ring. In contrast the B-ring of **2** is orientated at an angle to the NVP C ring with only one edge overlapping. There is no overlap of the C-ring of **2** with any part of NVP or EFV, while there is partial overlap with the indole ring of DLV (data not shown).

For EFV, the benzoxazinone ring partially overlaps the benzophenone ring B, but because the two rings are disposed at an angle, the common space occupied is relatively small. Nevertheless, particular individual substituents from the two inhibitors do overlap, e.g., the EFV cyclopropyl and trifluoromethyl groups with the **2** A-ring trifluoromethyl group and the B-ring chloro moiety, respectively.

Binding of 2−4 to Mutant RTs. We determined crystal structures of benzophenones in complex with known NNRTI drug resistance mutant RTs in order to assess whether these data would provide insight into compound resilience with such mutants. In particular, we wished to evaluate whether conformational flexibility could allow adaptation of the inhibitor to the mutant binding site. We therefore determined structures of complexes of **2** with the clinically important K103N mutant RT as well as for the double mutant V106A-Y181C (parts a and b of Figure 4). Overlapping of wild-type and K103N RT complexes with **2** showed an overall rms displacement of 0.3Å in the position of the inhibitor, which is close to the error of the coordinates. There are no significant differences in torsion angles for the groups linking rings A−B and B−C; thus, there is little evidence for **2** adapting to the mutated NNRTI site by flexing. Additionally, there are, generally, only small movements of the protein, e.g., a rotation of the position of the side chain

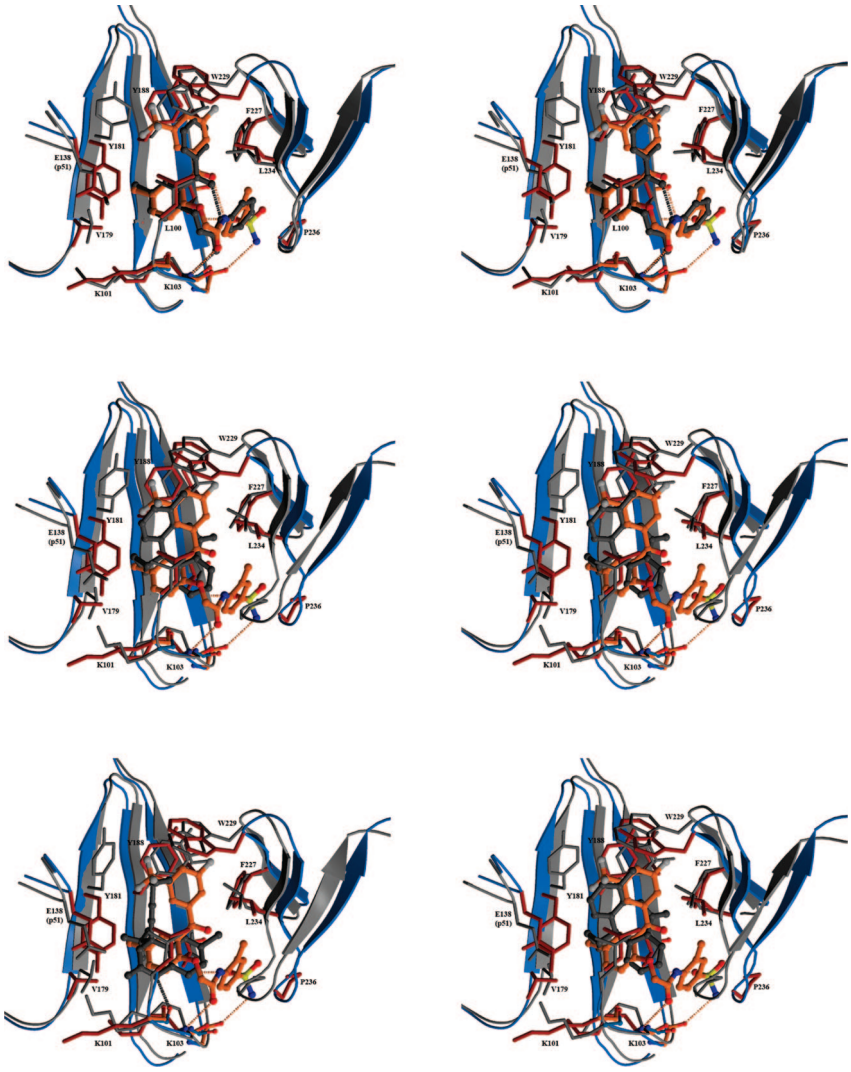

Figure 3. Stereodiagrams showing overlap of **2** and other inhibitors bound at the NNRTI site: (a, top) **2** and **1**; (b, middle) **2** and NVPl (c, bottom) **2** and EFV. For the complex with **2** the protein backbone is colored blue with interacting side chains colored red and the inhibitor colored by atoms. For other inhibitor complexes (**1**, NFV, and EFV) the protein backbone and interacting side chains are in light-gray and the inhibitor is in dark-gray. Hydrogen bonds are shown as broken lines.

of Y181 is observed. Comparing the overlapped complexes of **2** with wild-type and the double mutant V106A-Y181C RT reveals a larger shift in position of the inhibitor compared to that seen for the single K103N mutant (rms distance of 0.5 Å compared to 0.3 Å). Again, however, there are only minimal differences in the interaromatic ring torsion angles. The relative shift in atom positions between the two inhibitors can be accounted for by a small translation of the drug molecule. Even for this double mutant there is no evidence for **2** flexing in response to the presence of these drug resistance mutations in RT.

Neither **3** nor its prodrug **4** gave crystals with wild-type HIV-1 RT that were large enough to yield X-ray diffraction data to a useful resolution. Interestingly, in both cases suitable cocrystals for each of these compounds in complexes with single point mutant forms of RT were obtained (**3** with K103N and **4** with L100I). Assessment of the possible effects of mutations on the bound conformation of **3** and **4** is not entirely straightforward, as different mutations and small structural changes between drug and prodrug have to be considered. Overlaying **3** and **4** (when bound to RT K103N and RT L100I, respectively) shows slightly larger rearrangements than for **2** in mutant RTs (Figure 4c). There is a shift in the B-ring of ~0.6 Å away from residue 100. The propionyl tail group of **4** is positioned between the side chains of P225 and P236 with closest approach of 3.3 and 3.4 Å, respectively. The presence of the propionyl group and its location in a solvent accessible region with minimal conformational restraints is the likely cause of a rotation of the sulfonamide group of **4**. However, the largest changes are in the protein itself involving displacement of the loop region 96−101, with the biggest shift of 0.9 Å for the Cα atom of residue 99. Some changes in certain side chain positions including F227, V108, and L234 are also observed. Taken together, these results provide no evidence for NNRTI conformational and positional adaptability generated by the presence of the particular mutations studied, which contrasts with the results for etravirine (ETV)[31] and analogue TMC278,[33] where significant rearrangements were observed. In both K103N RT mutant structures there are additional van der Waals contacts present between the mutated side chain N103 and the edge of the B-ring for both **2** and **3**. These interactions involve hydrophilic atom(s) (either NH_2 but more likely O) from the side chain amide group to the hydrophobic aromatic ring. It is thus unclear if such interactions have significant compensatory

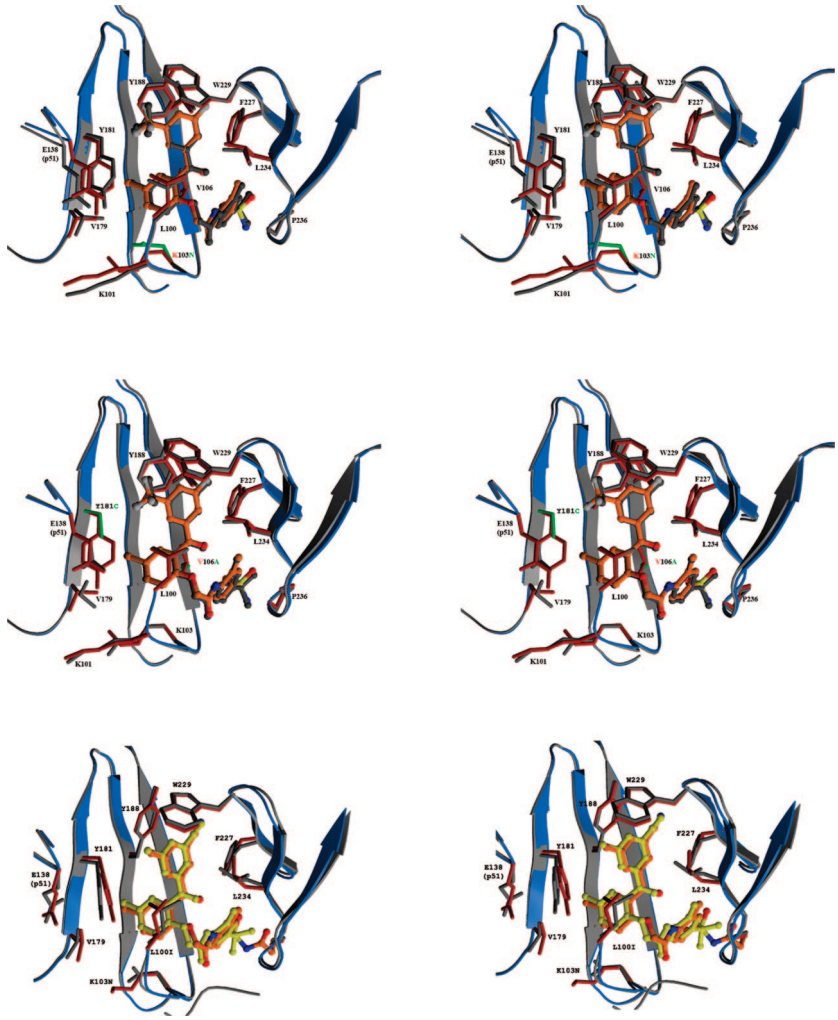

Figure 4. Stereodiagrams showing overlap of **2** and other inhibitors bound at mutated NNRTI sites: (a, top) **2** bound to wild-type and K103N RT; (b, middle) **2** bound to wild-type and Y181C-V106A RT; (c, bottom) **3** bound to K103N RT and **4** bound to L100I RT. The RT backbone is shown schematically and colored blue (wild-type) and gray (mutant). **2** is colored by atoms (wild-type) and gray (K103N). The site of the mutated side chain is colored in magenta for wild-type and green for the mutant. Hydrogen bonds are shown as broken lines.

effects to offset the stabilization of the unliganded enzyme induced by the K103N mutation H-bonding to the Y188 hydroxyl.

Predicting the Structural Basis for Benzophenone Resistance To Escape Mutations Generated in Vitro. Passaging HIV in tissue culture in the presence of 45nM **3** has been previously reported to select for a series of RT mutations including V106I, E138K, P236L in one experiment and K102E, V106A, and P236L in a second passage series.[27] A set of three mutations was required to give significant levels of resistance to **3**. Examination of the structures of **2** and **3** bound to RT provides indications of possible structural factors for the observed drug resistance in each case. For P236L, there is a loss of side chain contact with the C-ring in a manner similar to that predicted for the indole group of DLV.[34] The K102E mutation could act to disrupt a van der Waals contact of the lysine side chain CG atom with the carbonyl oxygen of the inhibitor linker region. The side chain of K102 forms a hydrogen bond from the lysine NE group to the main-chain carbonyl oxygen of P236. This hydrogen bond would be broken by the mutation of K102E, thereby potentially destabilizing the loop region and hence weakening the interaction of the P236 side chain interaction with the benzophenone C-ring. The V106A mutation would cause the loss of van der Waals contact with both the benzophenone B- and C-rings. Although there is a small shift in the position of **2** in the V106A/Y181C mutant, this does not restore the interactions seen with the wild-type protein. For V106I the opposite effect to V106A, an increase in bulk is likely to cause steric crowding and displacement of the B- and C-rings. The structural mechanism of resistance for the E138K mutation is likely to be more complex. The side chain E138 (p51) is positioned close to Y181 by virtue of the latter's unusual "down" position. A further consequence of this positioning is that the salt bridge between E138K and K101E (p66) observed in other RT structures appears much weaker, as the distance between the two groups is increased to 6.7 Å. Nevertheless, mutation of E138K, which introduces a longer side chain, will result in the juxtaposition of like (positive) charges (K101 and K138) which will therefore move apart. Such movements have previously been observed for this same E138K mutation in NVP complexes with RT.[22] In turn, the movement of K138 could allow release of Y181, which would result in the loss of van der Waals contact with the B-ring chloro substituent.

Structural Basis for Resilience of 2−4 to NNRTI Resistance Mutations. The structural data we report here suggest a number of factors that contribute to the remarkable resilience of new generation benzophenones such as **2**, **3**, and **4** to a wide range of known NNRTI resistance mutations. First, targeting the highly conserved W229 by introducing meta-substiuents onto ring A has the desired effect of reducing the contacts with the highly

mutable tyrosine residues 181 and 188. While we had previously observed increased binding resulting from the introduction of dimethyl substituents on the benzyl ring of emivirine analogue, **5** (GCA-186),[28] the structural effects on inhibitor positioning and protein conformation were less profound. Thus, the unexpected Y181 rearrangement to a "down" position was not previously observed in the case of **5** binding to RT. This rotameric flip for the wild-type Y181 side chain appears to result from one meta substituent on the A-ring of **2** and **3** pointing directly toward Y181, and the steric clash is such as to induce a "down" position. This "down" position for Y181 in the complexes of RT with **2** is more typical of the enzyme in the absence of NNRTIs (where Y188 is also in a "down" position) and has the effect of dramatically reducing the aromatic ring stacking contacts with **2**, although compensatory changes are seen such as the B-ring chloro substituent. Previous data indicated that the "up" position for Y181 was required for tight binding of first generation NNRTIs via induction of favorable aromatic ring stacking interactions.[35] Insufficient bulk at the 5-position of the HEPT[35] pyrimidine ring does not allow positioning of the Y181 side chain necessary for this optimal interaction with the inhibitor, explaining the weak binding of this compound. It appears that a variety of groups in other NNRTI series located in the correct position can trigger this rearrangement of the Y181 side chain. There are, however, a few other examples of Y181 being orientated in a "down" position in crystal structures.[18,36,37] Two of these structures are in the context of drug resistant mutant RTs where there may be some perturbation of the NNRTI pocket: EFV in K103N RT[18] and the NVP analogue 1051U91[36] bound to the azidothymidine resistant 4-mutant RTMC. Previous data have indicated a general mechanism of resistance for first generation NNRTIs such as NVP involving an indirect component whereby mutations disrupt the important inhibitor ring stacking interactions with Y181 and Y188 side chains.[20]

The presence of the A-ring meta-substituent and its interaction with RT also provides insight into the resilience of these compounds to mutation at residue 181. In both the wild-type and Y181C proteins, the meta-substituent would form van der Waals contact with the side chain of residue 181. With respect to Y188, the A-ring is able to stack imperfectly with the aromatic ring of Y188. However, the meta-substituents generate additional van der Waals contacts with either wild-type Y188 or mutant Y188L. On inspection, these edgewise contacts look attenuated; however, they seem to be beneficial, perhaps in limiting the thermal motion of Y188 and W229. Further, on a cooperative level, one meta-substituent points between Y188, W229, and F227, thus contacting three side chains simultaneously. Without the meta-substituent, there is a small solvent window framed by Y188, W229, and F227. Further, F227 is an important residue in that it can form a "bridge" or chain of van der Waals contacts between the A-ring and the C-ring of the ligand, provided that those rings have substituents that can make van der Waals contact with F227 (A-ring meta-substituent, C-ring ortho-subsituent). Lastly, V106 bridges the A-ring and B-rings; if the V106A mutation occurs, the bridging effect of F227 will tend to hold the ligand in place. This is apparently a structural feature that compensates for the V106 mutation. The affinity involved in these networks of van der Waals contacts is surely important for stabilizing both wild-type and mutant complexes.

For benzophenones such as **2**, where aromatic ring stacking interactions with Y181 are minimized compared to the prototype benzophenone **1**, there is a smaller contribution of the total binding energy derived from such contacts. Compensatory changes that do occur may in fact be more useful in maintaining activity against Y181C and certain other mutations. It is thus likely that the "down" position of the Y181 side chain represents a major contribution to the observed favorable resistance profile.

Additional contacts of **2** and **3** with the mutated side chain are present in the K103N RT structure. It is not clear as to what extent these interactions contribute to the improved activity of these compounds against the K103N mutant compared to the prototype **1** because of the potentially unfavorable nature of these hydrophobic−hydrophilic contacts. A further potentially important feature that could help explain the favorable resistance profile of **2** and **3** is the presence of up to four inhibitor-to-protein main-chain hydrogen bonds. While a single main-chain hydrogen bond is relatively common in the binding of many NNRTIs, the presence of three or more is unusual. In the case of capravirine or S-1153 (CPV), which has three H-bonds, it has a resilience profile that is significantly improved from that of EFV.[15,38] Such inhibitor to main-chain hydrogen bonding is less easily disrupted than side chain interactions by the introduction of mutations.

NNRTIs having significantly improved resistance profiles compared to first generation compounds such as NVP fall into two distinct structural categories. The first category has relatively low molecular weight compounds with a rigid core ring system such as EFV, **6** (HBY097),[19] and **7** (GW420867X).[39] While substituents on the EFV ring system are generally also rigid, those of **6** and **7** have more flexibility. Such inhibitors have the ability to rearrange their position within the NNRT pocket in response to the presence of certain drug resistance mutations. In each case, these inhibitors have a relatively small component of their binding energy derived from contacts with Y181; hence, rearrangement has less of a penalty resulting from the loss of ring stacking interactions. The second category compounds have a higher molecular weight than EFV/**7** and usually contain three aromatic rings joined by linker groups; these include CPV,[38] ETV,[31] and the current benzophenone series. For ETV, it is reported to undergo conformational and positional adaptation within the NNRTI binding site, referred to as "wiggling" and "jiggling", in response to the presence of drug resistance mutations.[31] In the case of the current benzophenone series, **2** shows minimal such conformational and positional adaptation in response to a single and double mutation in RT. For **3** bound to the mutant L100I RT there is evidence for more significant conformational differences, but these are biggest for the protein itself rather than the drug molecule. Thus, despite some apparent structural similarity, it seems likely that significantly different mechanisms may account for the common feature of resilience to drug resistance mutations with these newer generation NNRTIs. The possibility of such a variety of different mechanisms is encouraging, as it implies there are several ways of developing novel compounds with improved resistance profiles.

Conclusions

The fact that drug resistant virus can be readily selected remains a significant problem in maintaining effective treatment of HIV-infected individuals. The development of new drugs with activity profiles to include the wide range of HIV mutants encoding resistance for that particular inhibitor class is thus essential. The structural studies of the benzophenone series of NNRTIs bound to RT were undertaken as part of a combined approach to design a new generation of benzophenone NNRTIs with a greatly improved resistance profiles. Structure determination of prototype and later stage benzophenone NNRTIs identified factors that can contribute to the improved resilience

of the optimized compounds. Understanding such mechanisms underlying the maintenance of high potency of benzophenones against a wide range of mutant RTs is potentially of wider importance for the design of further NNRTIs from different chemical series. Such efforts are of vital importance for the development of novel drugs for use in the continued treatment of HIV and AIDS.

Experimental Section

Enzyme and Inhibitor Preparation. Expression vectors for HIV-1 RT cloned from an HXB-2 isolate, both wild-type and NNRTI drug resistant mutant forms, were constructed as previously described.[17] Wild-type and mutant RTs were expressed in *E. coli* and purified using the ion-exchange and gel filtration based procedures as used in an earlier study.[40] Benzopheneone NNRTIs **1**, **2**, **3**, and the latter's prodrug **4** were synthesized and characterized as reported in earlier papers.[23−26]

Anti-HIV-1 Activity and Resistance Profile of 1 in Cell Culture Systems. The anti-HIV-1 activity of the prototype benzophenone **1** was tested against a wider panel of mutant viruses than previously reported[23] using the methods described in earlier studies.[25,27] For comparative purposes, antiviral data for benzophenones **2** and **3** and reference drugs NVP, DLV, and EFV were obtained against the same panel of mutant viruses. Numerical data are shown in Supporting Information Table 1.

Crystallization and Data Collection. Cocrystallization trials of wild-type, various single point mutant (e.g., L100I, K101E, K103N, V106A, V108I, E138K, Y181C, Y188C), or double mutation (such as V106A -Y181C) RTs with different benzophenone NNRTIs were set up using conditions previously reported.[41] Crystals were subjected to a gradual increase in PEG 3400 concentration to a maximum of 50% (w/v) prior to data collection. This partial dehydration protocol significantly improved the diffraction limit of the crystals.[41,42] The structures of complexes of RT and benzophenones reported here were all from cocrystallizations and not derived by displacement of weak binding inhibitors using soaking experiments. X-ray data were collected at synchrotron: the ESRF, Grenoble, France and the SRS, Daresbury, U.K. Liquid propane was used to flash-cool crystals, which were then maintained at 100 K in a nitrogen gas stream during data collection. Data images were indexed and integrated using DENZO; data merging was with SCALEPACK.[43] Details of the X-ray data statistics are given in Table 1.

Structure Solution and Refinement. All structures were solved by molecular replacement using rigid body refinement in CNS.[44] The choice of starting model from our database of RT-NNRTI complexes was decided for each particular structure determination as judged by the closeness of unit cell parameters.[10,12−14,17,18,28,35] Positional, simulated annealing, and individual *B*-factor refinement with bulk solvent correction and anisotropic *B*-factor scaling was then carried out using CNS.[44] Model rebuilding was carried out on a molecular graphics workstation using "O".[45] Table 1 gives the refinement statistics for the six RT−benzophenone structures reported here.

Structures of wild-type and mutant RTs were overlapped by the program SHP[46] using 110 residues that form a relatively rigid core region. The wild-type RT complexes used for these comparisons were 1rtd (for NVP)[10] and 1fk9 (for EFV).[47]

Acknowledgment. We thank the staff of the following synchrotrons for their assistance in data collection: The Synchrotron Radiation Source, Daresbury, U.K and the European Synchrotron Radiation Facility, Grenoble, France. Financial support via grants from the Medical Research Council, the Biotechnology and Biological Sciences Research Council, and the EC (Grants QLKT-2000-00291 and QLKT2-CT-2002-01311) to D.K.S. is acknowledged.

Supporting Information Available: Numeric antiviral data used for Figure 1. This material is available free of charge via the Internet at http://pubs.acs.org.

References

(1) De Clercq, E. New developments in anti-HIV chemotherapy. *Curr. Med. Chem.* **2001**, *8*, 1543–1572.
(2) Reed, C.; Daar, E. S. Novel antiretroviral agents in HIV therapy. *Curr. Infect. Dis. Rep.* **2006**, *8*, 489–496.
(3) Kohlstaedt, L. A.; Wang, J.; Friedman, J. M.; Rice, P. A.; Steitz, T. A. Crystal structure at 3.5 Å resolution of HIV-1 reverse transcriptase complexed with an inhibitor. *Science* **1992**, *256*, 1783–1790.
(4) Huang, H.; Chopra, R.; Verdine, G. L.; Harrison, S. C. Structure of a covalently trapped catalytic complex of HIV-1 reverse transcriptase: implications for drug resistance. *Science* **1998**, *282*, 1669–1675.
(5) Goody, R. S.; Muller, B.; Restle, T. Factors contributing to the inhibition of HIV reverse transcriptase by chain-terminiating nucleotides in vivo. *FEBS Lett.* **1991**, *291*, 1–5.
(6) Esnouf, R.; Ren, J.; Ross, C.; Jones, Y.; Stammers, D.; Stuart, D. Mechanism of inhibition of HIV-1 reverse transcriptase by nonnucleoside inhibitors. *Nat. Struct. Biol.* **1995**, *2*, 303–308.
(7) Spence, R. A.; Kati, W. M.; Anderson, K. S.; Johnson, K. A. Mechanism of inhibition of HIV-1 reverse transcriptase by nonnucleoside inhibitors. *Science* **1995**, *267*, 988–993.
(8) Schinazi, R. F.; Larder, B. A.; Mellors, J. W. Mutations in retroviral genes associated with drug resistance. *Int. Antiviral News* **2000**, *8*, 65–71.
(9) Young, S. D.; Britcher, S. F.; Tran, L. O.; Payne, L. S.; Lumma, W. C.; Lyle, T. A.; Huff, J. R.; Anderson, P. S.; Olsen, D. B.; Carroll, S. S.; Pettibone, D. J.; O'Brien, J. A.; Ball, R. G.; Balani, S. K.; Lin, J. H.; Chen, I.-W.; Schleif, W. A.; Sardana, V. V.; Long, W. J.; Byrnes, V. W.; Emini, E. A. L-743,726 (DMP-266): a novel, highly potent nonnucleoside inhibitor of the human immunodeficiency virus type 1 reverse transcriptase. *Antimicrob. Agents Chemother.* **1995**, *39*, 2602–2605.
(10) Ren, J.; Esnouf, R.; Garman, E.; Somers, D.; Ross, C.; Kirby, I.; Keeling, J.; Darby, G.; Jones, Y.; Stuart, D.; Stammers, D. High resolution structures of HIV-1 RT from four RT−inhibitor complexes. *Nat. Struct. Biol.* **1995**, *2*, 293–302.
(11) Ding, J.; Das, K.; Moereels, H.; Koymans, L.; Andries, K.; Janssen, P. A. J.; Hughes, S. H.; Arnold, E. Structure of HIV-1 RT/TIBO R 86183 complex reveals similarity in the binding of diverse nonnucleoside inhibitors. *Nat. Struct. Biol.* **1995**, *2*, 407–415.
(12) Ren, J.; Esnouf, R.; Hopkins, A.; Ross, C.; Jones, Y.; Stammers, D.; Stuart, D. The structure of HIV-1 reverse transcriptase complexed with 9-chloro-TIBO: lessons for inhibitor design. *Structure* **1995**, *3*, 915–926.
(13) Ren, J.; Esnouf, R. M.; Hopkins, A. L.; Stuart, D. I.; Stammers, D. K. Crystallographic analysis of the binding modes of thiozolo-isoindolinone non-nucleoside inhibitors to HIV-1 reverse transcriptase and comparison with modelling studies. *J. Med. Chem.* **1999**, *42*, 3845–3851.
(14) Ren, J.; Esnouf, R. M.; Hopkins, A. L.; Warren, J.; Balzarini, J.; Stuart, D. I.; Stammers, D. K. Crystal structures of HIV-1 reverse transcriptase in complex with carboxanilide derivatives. *Biochemistry* **1998**, *37*, 14394–14403.
(15) Ren, J.; Nichols, C. E.; Bird, L. E.; Fujiwara, T.; Sugimoto, H.; Stuart, D. I.; Stammers, D. K. Binding of the second generation nonnucleoside inhibitor S-1153 to HIV-1 RT involves extensive main chain hydrogen bonding. *J. Biol. Chem.* **2000**, *275*, 14316–14320.
(16) Das, K.; Ding, J.; Hsiou, Y.; Clark, A. D.; Moereels, H.; Koymans, L.; Andries, K.; Pauwels, R.; Janssen, P. A.; Boyer, P. L.; Clark, P.; Smith, R. H.; Kroeger Smith, M. B.; Michejda, C. J.; Hughes, S. H.; Arnold, E. Crystal structures of 8-Cl and 9-Cl TIBO complexed with wild-type HIV-1 RT and 8-Cl TIBO complexed with the Tyr181Cys HIV-1 RT drug-resistant mutant. *J. Mol. Biol.* **1996**, *264*, 1085–1100.
(17) Ren, J.; Nichols, C.; Bird, L.; Chamberlain, P.; Weaver, K.; Short, S.; Stuart, D. I.; Stammers, D. K. Structural mechanisms of drug resistance for mutations at codons 181 and 188 in HIV-1 reverse transcriptase and the improved resilience of second generation nonnucleoside inhibitors. *J. Mol. Biol.* **2001**, *312*, 795–805.
(18) Ren, J.; Milton, J.; Weaver, K. L.; Short, S. A.; Stuart, D. I.; Stammers, D. K. Structural basis for the resilience of efavirenz (DMP-266) to drug resistance mutations in HIV-1 reverse transcriptase. *Structure* **2000**, *8*, 1089–1094.
(19) Hsiou, Y.; Das, K.; Ding, J.; Clark, A. D.; Kleim, J.-P.; Rosner, M.; Winkler, I.; Riess, G.; Hughes, S. H.; Arnold, E. HIV-1 reverse transcriptase complexed with the non-nucleoside inhibitor HBY 097: inhibitor flexibility is a useful design feature for reducing drug resistance. *J. Mol. Biol.* **1998**, *284*, 313–323.

(20) Ren, J.; Nichols, C. E.; Chamberlain, P. P.; Weaver, K. L.; Short, S. A.; Stammers, D. K. Crystal structures of HIV-1 reverse transcriptase mutated at codons 100, 106 and 108 and mechanisms of resistance to non-nucleoside inhibitors. *J. Mol. Biol.* **2004**, *336*, 569–578.

(21) Lindberg, J.; Sigurosson, S.; Lowgren, S.; Andersson, H. O.; Sahlberg, C.; Noreen, R.; Fridborg, K.; Zhang, H.; Unge, T. Structural basis for the inhibitory efficacy of efavirenz (DMP-266), MSC194 and PNU142721 towards the HIV-1 RT K103N mutant. *Eur. J. Biochem.* **2002**, *269*, 1670–1677.

(22) Ren, J.; Nichols, C. E.; Stamp, A.; Chamberlain, P. P.; Ferris, R.; Weaver, K. L.; Short, S. A.; Stammers, D. K. Structural insights into mechanisms of non-nucleoside drug resistance for HIV-1 reverse transcriptases mutated at codons 101 or 138. *FEBS J.* **2006**, *273*, 3850–3860.

(23) Wyatt, P. G.; Bethell, R. C.; Cammack, N.; Charon, D.; Dodic, N.; Dumaitre, B.; Evans, D. N.; Green, D. V.; Hopewell, P. L.; Humber, D. C.; et al. Benzophenone derivatives: a novel series of potent and selective inhibitors of human immunodeficiency virus type 1 reverse transcriptase. *J. Med. Chem.* **1995**, *38*, 1657–1665.

(24) Chan, J. H.; Freeman, G. A.; Tidwell, J. H.; Romines, K. R.; Schaller, L. T.; Cowan, J. R.; Gonzales, S. S.; Lowell, G. S.; Andrews, C. W., 3rd; Reynolds, D. J.; St Clair, M.; Hazen, R. J.; Ferris, R. G.; Creech, K. L.; Roberts, G. B.; Short, S. A.; Weaver, K.; Koszalka, G. W.; Boone, L. R. Novel benzophenones as non-nucleoside reverse transcriptase inhibitors of HIV-1. *J. Med. Chem.* **2004**, *47*, 1175–1182.

(25) Ferris, R. G.; Hazen, R. J.; Roberts, G. B.; St Clair, M. H.; Chan, J. H.; Romines, K. R.; Freeman, G. A.; Tidwell, J. H.; Schaller, L. T.; Cowan, J. R.; Short, S. A.; Weaver, K. L.; Selleseth, D. W.; Moniri, K. R.; Boone, L. R. Antiviral activity of GW678248, a novel benzophenone nonnucleoside reverse transcriptase inhibitor. *Antimicrob. Agents Chemother.* **2005**, *49*, 4046–4051.

(26) Romines, K. R.; Freeman, G. A.; Schaller, L. T.; Cowan, J. R.; Gonzales, S. S.; Tidwell, J. H.; Andrews, C. W., 3rd; Stammers, D. K.; Hazen, R. J.; Ferris, R. G.; Short, S. A.; Chan, J. H.; Boone, L. R. Structure−activity relationship studies of novel benzophenones leading to the discovery of a potent, next generation HIV nonnucleoside reverse transcriptase inhibitor. *J. Med. Chem.* **2006**, *49*, 727–739.

(27) Hazen, R. J.; Harvey, R. J.; St Clair, M. H.; Ferris, R. G.; Freeman, G. A.; Tidwell, J. H.; Schaller, L. T.; Cowan, J. R.; Short, S. A.; Romines, K. R.; Chan, J. H.; Boone, L. R. Anti-human immunodeficiency virus type 1 activity of the nonnucleoside reverse transcriptase inhibitor GW678248 in combination with other antiretrovirals against clinical isolate viruses and in vitro selection for resistance. *Antimicrob. Agents Chemother.* **2005**, *49*, 4465–4473.

(28) Hopkins, A. L.; Ren, J.; Tanaka, H.; Baba, M.; Okamato, M.; Stuart, D. I.; Stammers, D. K. Design of MKC-442 (emivirine) analogues with improved activity against drug resistant HIV mutants. *J. Med. Chem.* **1999**, *42*, 4500–4505.

(29) Hopkins, A. L.; Ren, J.; Milton, J.; Hazen, R. J.; Chan, J. H.; Stuart, D. I.; Stammers, D. K. Design of non-nucleoside inhibitors of HIV-1 reverse transcriptase with improved drug resistance properties. 1. *J. Med. Chem.* **2004**, *47*, 5912–5922.

(30) Freeman, G. A.; Andrews, C. W., 3rd; Hopkins, A. L.; Lowell, G. S.; Schaller, L. T.; Cowan, J. R.; Gonzales, S. S.; Koszalka, G. W.; Hazen, R. J.; Boone, L. R.; Ferris, R. G.; Creech, K. L.; Roberts, G. B.; Short, S. A.; Weaver, K.; Reynolds, D. J.; Milton, J.; Ren, J.; Stuart, D. I.; Stammers, D. K.; Chan, J. H. Design of non-nucleoside inhibitors of HIV-1 reverse transcriptase with improved drug resistance properties. 2. *J. Med. Chem.* **2004**, *47*, 5923–5936.

(31) Das, K.; Clark, A. D., Jr.; Lewi, P. J.; Heeres, J.; De Jonge, M. R.; Koymans, L. M.; Vinkers, H. M.; Daeyaert, F.; Ludovici, D. W.; Kukla, M. J.; De Corte, B.; Kavash, R. W.; Ho, C. Y.; Ye, H.; Lichtenstein, M. A.; Andries, K.; Pauwels, R.; De Bethune, M. P.; Boyer, P. L.; Clark, P.; Hughes, S. H.; Janssen, P. A.; Arnold, E. Roles of conformational and positional adaptability in structure-based design of TMC125-R165335 (etravirine) and related non-nucleoside reverse transcriptase inhibitors that are highly potent and effective against wild-type and drug-resistant HIV-1 variants. *J. Med. Chem.* **2004**, *47*, 2550–2560.

(32) Pelemans, H.; Esnouf, R.; De Clercq, E.; Balzarini, J. Mutational analysis of trp-229 of human immunodeficiency virus type 1 reverse transcriptase (RT) identifies this amino acid residue as a prime target for the rational design of new non-nucleoside RT inhibitors. *Mol. Pharmacol.* **2000**, *57*, 954–960.

(33) Das, K.; Bauman, J. D.; Clark, A. D., Jr.; Frenkel, Y. V.; Lewi, P. J.; Shatkin, A. J.; Hughes, S. H.; Arnold, E. High-resolution structures of HIV-1 reverse transcriptase/TMC278 complexes: strategic flexibility explains potency against resistance mutations. *Proc. Natl. Acad. Sci. U.S.A.* **2008**, *105*, 1466–1471.

(34) Esnouf, R. M.; Stuart, D. I.; De Clercq, E.; Schwartz, E.; Balzarini, J. Models which explain the inhibition of reverse transcriptase by HIV-1-specific (thio)carboxanilide derivatives. *Biochem. Biophys. Res. Commun.* **1997**, *234*, 458–464.

(35) Hopkins, A. L.; Ren, J.; Esnouf, R. M.; Willcox, B. E.; Jones, E. Y.; Ross, C.; Miyasaka, T.; Walker, R. T.; Tanaka, H.; Stammers, D. K.; Stuart, D. I. Complexes of HIV-1 reverse transcriptase with inhibitors of the HEPT series reveal conformational changes relevant to the design of potent non-nucleoside inhibitors. *J. Med. Chem.* **1996**, *39*, 1589–1600.

(36) Ren, J.; Esnouf, R. M.; Hopkins, A. L.; Jones, E. Y.; Kirby, I.; Keeling, J.; Ross, C. K.; Larder, B. A.; Stuart, D. I.; Stammers, D. K. 3′-Azido-3′-deoxythymidine drug resistance mutations in HIV-1 reverse transcriptase can induce long range conformational changes. *Proc. Natl. Acad. Sci. U.S.A.* **1998**, *95*, 9518–9523.

(37) Himmel, D. M.; Das, K.; Clark, A. D., Jr.; Hughes, S. H.; Benjahad, A.; Oumouch, S.; Guillemont, J.; Coupa, S.; Poncelet, A.; Csoka, I.; Meyer, C.; Andries, K.; Nguyen, C. H.; Grierson, D. S.; Arnold, E. Crystal structures for HIV-1 reverse transcriptase in complexes with three pyridinone derivatives: a new class of non-nucleoside inhibitors effective against a broad range of drug-resistant strains. *J. Med. Chem.* **2005**, *48*, 7582–7591.

(38) Fujiwara, T.; Sato, A.; el-Farrash, M.; Miki, S.; Abe, K.; Isaka, Y.; Kodama, M.; Wu, Y.; Chen, L. B.; Harada, H.; Sugimoto, H.; Hatanaka, M.; Hinuma, Y. S-1153 inhibits replication of known drug-resistant strains of human immunodeficiency virus type 1. *Antimicrob. Agents Chemother.* **1998**, *42*, 1340–1345.

(39) Balzarini, J.; De Clercq, E.; Carbonez, A.; Burt, V.; Kleim, J. P. Long-term exposure of HIV type 1-infected cell cultures to combinations of the novel quinoxaline GW420867X with lamivudine, abacavir, and a variety of nonnucleoside reverse transcriptase inhibitors. *AIDS Res. Hum. Retroviruses* **2000**, *16*, 517–528.

(40) Wilson, J. E.; Wright, L. L.; Martin, J. L.; Haire, S. E.; Ray, P. H.; Painter, G. R.; Furman, P. A. Recombinant human immunodeficiency virus type 1 reverse transcriptase is heterogeneous. *J. Acquired Immune Defic. Syndr. Hum. Retrovirol.* **1996**, *11*, 20–30.

(41) Stammers, D. K.; Somers, D. O. N.; Ross, C. K.; Kirby, I.; Ray, P. H.; Wilson, J. E.; Norman, M.; Ren, J. S.; Esnouf, R. M.; Garman, E. F.; Jones, E. Y.; Stuart, D. I. Crystals of HIV-1 reverse transcriptase diffracting to 2.2Å resolution. *J. Mol. Biol.* **1994**, *242*, 586–588.

(42) Esnouf, R. M.; Ren, J.; Garman, E. F.; Somers, D. O. N.; Ross, C. K.; Jones, E. Y.; Stammers, D. K.; Stuart, D. I. Continuous and discontinuous changes in the unit cell of HIV-1 reverse transcriptase crystals on dehydration. *Acta Crystallogr.* **1998**, *D54*, 938–954.

(43) Otwinowski, Z.; Minor, W. Processing of X-ray diffraction data collected in oscillation mode. *Methods Enzymol.* **1996**, *276*, 307–326.

(44) Brunger, A. T.; Adams, P. D.; Clore, G. M.; Delano, W. L.; Gros, P.; Grosse, K. R. W.; Jiang, J. S.; Kuszewski, J.; Nilges, M.; Pannu, N. S.; Read, R. J.; Rice, L. M.; Simonson, T.; Warren, G. L. Crystallography and NMR system: a new software suite for macromolecular structure determination. *Acta Crystallogr.* **1998**, *D54*, 905–921.

(45) Jones, T. A.; Zou, J. Y.; Cowan, S. W.; Kjeldgaard, M. Improved methods for building protein models in electron density maps and the location of errors in these models. *Acta Crystallogr.* **1991**, *A47*, 110–119.

(46) Stuart, D. I.; Levine, M.; Muirhead, H.; Stammers, D. K. The crystal structure of cat pyruvate kinase at a resolution of 2.6 Å. *J. Mol. Biol.* **1979**, *134*, 109–142.

(47) Ren, J.; Diprose, J.; Warren, J.; Esnouf, R. M.; Bird, L. E.; Ikemizu, S.; Slater, M.; Milton, J.; Balzarini, J.; Stuart, D. I.; Stammers, D. K. Phenylethylthiazolylthiourea (PETT) non-nucleoside inhibitors of HIV-1 and HIV-2 reverse transcriptases: structural and biochemical analyses. *J. Biol. Chem.* **2000**, *275*, 5633–5639.

JM8004493